

Charmless B decays: 2 body and $B \rightarrow VV$

Cibrán Santamarina Ríos* †

Universidade de Santiago de Compostela

E-mail: cibran.santamarina@usc.es

Charmless decays of B mesons provide powerful probes for physics beyond the Standard Model. The latest results of the LHCb collaboration on the pseudo-scalar-vector $B_s^0 \rightarrow K^{*\pm} h^\mp$ and vector-vector $B^0 \rightarrow \phi K^{*0}$ and $B_s^0 \rightarrow \phi \phi$ final states with data samples of the LHC RUN-I are presented.

*The 15th International Conference on B-Physics at Frontier Machines at the University of Edinburgh,
14 -18 July, 2014
University of Edinburgh, UK*

*Speaker.

†for the LHCb collaboration.

1. Introduction

The weak interaction flavour changing transitions provide the only mechanism that breaks the CP symmetry within the Standard Model (SM). Such transitions of quarks are described by the CKM matrix [1]. The hierarchy of the CKM matrix establishes that the most favoured flavour transitions are those that take place between two consecutive quark families. Charmless decays of B mesons are among the most interesting probes of physics beyond the SM in flavour-changing reactions since they can only occur through $b \rightarrow u$ tree transitions, that connect the third and first quark families, and loop mediated $b \rightarrow s$ or $b \rightarrow d$ transitions.

The presented results have been achieved by the LHCb collaboration analysing all or a sub-sample of the data provided by proton-proton collisions of the Large Hadron Collider at CERN. More details of the analyses can be found in Refs. [2], [3] and [4].

The accumulated LHCb data sample amounts to $1 fb^{-1}$ integrated luminosity in 2011, at $\sqrt{s} = 7 TeV$ centre of mass energy, and $2 fb^{-1}$ integrated luminosity in 2012 at $\sqrt{s} = 8 TeV$. The LHCb detector [5] is a single-arm forward spectrometer covering the pseudorapidity range $2 < \eta < 5$, that benefits from the low angle production of $b\bar{b}$ pairs in the LHC pp collisions. The cross section of these pairs is, at $\sqrt{s} = 7 TeV$, $284 \pm 53 mb$ [13], a factor of 10^4 higher than the production rate at the B -factories. The detector includes a high-precision tracking system [6], that provides a measurement of momentum with a relative uncertainty that varies from 0.4% at low momentum to 0.6% at $100 GeV/c$. and a resolution of $(15 + 29/p_t)\mu m$ ¹ in the impact parameter resolution. These specifications allow optimal reconstruction of displaced vertexes of heavy particle decays needed for identification of B meson decays. Different types of charged hadrons are distinguished using information from two ring-imaging Cherenkov detectors [7]. Photon, electron and hadron candidates are identified by a calorimeter system and muons are distinguished by a system composed of alternating layers of iron and multiwire proportional chambers [8].

2. Observation of $B_s^0 \rightarrow K^{*\pm}K^\mp$ and evidence for $B_s^0 \rightarrow K^{*-}\pi^+$ decays

Direct CP violation is the most evident manifestation of CP violation. This consists of asymmetries in the partial widths of CP reversed decays with contributions from interfering amplitudes with different weak and strong phases. Large CP violation asymmetries of $\mathcal{O}(10\%)$ or more between the rates of \bar{B} and B meson decays to CP conjugate final states, have been observed in $B^0 \rightarrow K^+\pi^-$ and $B_s^0 \rightarrow K^-\pi^+$ [9] and $B^+ \rightarrow \pi^+\pi^-K^+$, $K^+K^-K^+$, $\pi^+\pi^-\pi^+$ and $K^+K^-\pi^+$ decays [10]. It is hard to be certain whether these asymmetries originate in the weak interaction or beyond the SM due to the presence of parameters describing the hadronic interactions that are difficult to determine either theoretically or from data. An approach to control the hadronic uncertainties is to study the distribution of kinematic configurations of $B_d^0 \rightarrow K_S^0\pi^+\pi^-$ decays across the Dalitz plot [11]. In this way the relative phase between the Pseudoscalar-Vector (PV) $K^{*+}\pi^-$ and $K_S^0\rho^0$ amplitudes can be determined. This information is not accessible in studies either of two-body decays, or of the inclusive properties of three-body decays.

Different methods to test the SM with B meson decays to charmless PV (πK^* and $K\rho$) states have been proposed [12] that require the experimental input of the magnitudes and relative phases

¹ p_t is the component of particle momentum transverse to the beam, in GeV/c .

of the decay amplitudes. Although the phases can only be obtained from Dalitz plot analyses of B meson decays to final states containing one kaon and two pions, the magnitudes can be obtained from simplified approaches. Decays of B mesons to K^*K final states can be studied with similar methods. This motivates the study of B meson decays into K^*h , where h is either a pion or a kaon. These proceedings summarise the first measurements of B_s^0 meson decays to $K^{*-}\pi^+$ and $K^{*\pm}K^\mp$ final states and the $B^0 \rightarrow K^{*\pm}K^\mp$ rate.

The presented results were obtained with the 2011 LHC data sample, which is too small for a detailed Dalitz plot analysis, and therefore only branching fractions are measured. A full analysis will be possible with the larger data samples that will be recorded in the following years. The $K^{*\pm}$ mesons are reconstructed in their decays to $K_S^0\pi^\pm$ with $K_S^0 \rightarrow \pi^+\pi^-$. The event selection is optimised based on the expected level of background within the allowed $K_S^0\pi^\pm$ mass window. The singular topology of K_S^0 meson decays, with their long lifetimes, produces two categories of events: *long*, where both tracks from the $K_S^0 \rightarrow \pi^+\pi^-$ decay contain hits in the Vertex Locator (VELO) of LHCb, and *downstream*, where neither does. Both categories have associated hits in the tracking detectors downstream of the magnet. *Long* candidates have better mass and vertex resolution and consequently, different selection requirements are imposed for the two categories.

A multivariate selection method is trained for the suppression of combinatorial background and backgrounds from B meson decays with charm or charmonia in the intermediate state and other hadron decays that can contaminate the signal.

An unbinned maximum likelihood fit in the two dimensions in ranges $5000 < m(K_S^0h^\pm\pi^\mp) < 5500 \text{ MeV}/c^2$ and $650 < m(K_S^0\pi^\mp) < 1200 \text{ MeV}/c^2$ of the B and K^* candidates invariant masses is employed to distinguish signal from background of the final selected sample. This approach allows the resonant $B^0 \rightarrow K^{*\pm}h^\mp$ decay to be separated from other B meson decays to the $K_S^0\pi^\pm h^\mp$ final state. However, it does not account for interference effects between the $K^{*\pm}h^\mp$ component and other amplitudes contributing to the Dalitz plot; possible biases due to this assumption are considered as a source of systematic uncertainty.

The B meson candidate mass spectrum accounts for the following contributions: B^0 and B_s^0 signal, B^0 and B_s^0 non-resonant components, misidentified $B^0 \rightarrow K^{*\pm}h^\mp$ cross-feed, backgrounds from charmless decays with missing particles: $\Lambda_b^0 \rightarrow K^{*-}p$ and $B^+ \rightarrow D^0(\rightarrow K_S^0\pi^+\pi^-)h^+$ and combinatorial background.

The yields for the different signal channels are summarised in Table 1 and the *downstream* spectra are shown in Figure 2. These yields translate into the measurement of the decay modes $B_s^0 \rightarrow K^{*\pm}K^\mp$ with 12.5 and $B_s^0 \rightarrow K^{*-}\pi^+$ with 3.9 standard deviations significance. The observed signal significance for the decay $B^0 \rightarrow K^{*\pm}K^\mp$ is below 2σ .

With the obtained yields the branching fractions are determined using the $B^0 \rightarrow K^{*\pm}\pi^\mp$ mode² as a reference:

$$\begin{aligned}\mathcal{B}(B_s^0 \rightarrow K^{*\pm}K^\mp) &= (12.7 \pm 1.9 \text{ stat} \pm 1.9 \text{ syst}) \times 10^{-6}, \\ \mathcal{B}(B^0 \rightarrow K^{*\pm}K^\mp) &= (0.17 \pm 0.15 \text{ stat} \pm 0.05 \text{ syst}) \times 10^{-6}, \\ &< 0.4 (0.5) \times 10^{-6} \text{ at } 90\% (95\%) \text{ CL}, \\ \mathcal{B}(B_s^0 \rightarrow K^{*-}\pi^+) &= (3.3 \pm 1.1 \text{ stat} \pm 0.5 \text{ syst}) \times 10^{-6}.\end{aligned}$$

²The branching fraction of this mode is $\mathcal{B}(B^0 \rightarrow K^{*\pm}\pi^\mp) = (8.5 \pm 0.7) \times 10^{-6}$ [14].

Table 1: Yields and relative yields obtained from the fits to $K^{*\pm}K^\mp$ and $K^{*\pm}\pi^\mp$ candidates. The relative yields of nonresonant (NR) $B_{(s)}^0$ decays are constrained to be identical in *long* and *downstream* categories. Only statistical uncertainties are given.

| Yield | B^0 | | B_s^0 | |
|---|-----------------|-------------------|-----------------|-------------------|
| | <i>long</i> | <i>downstream</i> | <i>long</i> | <i>downstream</i> |
| $N(K^{*\pm}K^\mp)$ | 0 ± 4 | 4 ± 3 | 40 ± 8 | 62 ± 10 |
| $N(K^{*\pm}\pi^\mp)$ | 80 ± 10 | 165 ± 16 | 5 ± 4 | 23 ± 8 |
| $N(K_S^0\pi^\pm K^\mp \text{NR})/N(K^{*\pm}K^\mp)$ | 0.0 ± 1.0 | | 0.41 ± 0.16 | |
| $N(K_S^0\pi^\pm\pi^\mp \text{NR})/N(K^{*\pm}\pi^\mp)$ | 0.79 ± 0.14 | | 0.6 ± 0.4 | |

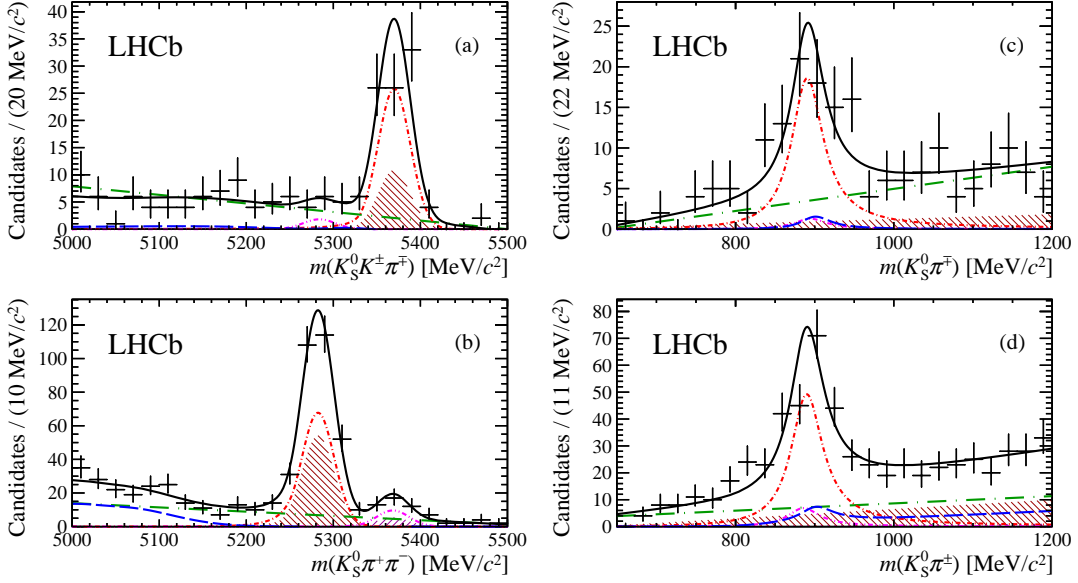


Figure 1: Results of the fit to $K^{*\pm}h^\mp$ downstream candidates projected onto (a,b) B candidate and (c,d) K^* candidate mass distributions, for (a,c) $K^{*\pm}K^\mp$ and (b,d) $K^{*\pm}\pi^\mp$ candidates. The total fit result (solid black line) is shown together with the data points. Components for the B^0 (pink dash double-dotted line) and B_s^0 (red dash dotted line) signals are shown together with the B_s^0 nonresonant component (dark red falling hatched area), charmless partially reconstructed and cross-feed background (blue long-dashed line), and combinatorial background (green long-dash dotted line) components.

3. $B_{(s)}^0 \rightarrow VV'$ penguins

Penguin decays of B mesons are dominated by Feynman diagrams in which a virtual t quark, the heaviest SM elementary particle, is exchanged forming a loop with a W boson. Since the SM predicts a small CP violating weak phase in the product of CKM matrix elements for loop-induced $b \rightarrow s$ transitions, any observed deviation could indicate physics beyond the SM possibly mediated by a particle with a mass comparable or higher than that of the t -quark. See few examples in Ref. [15]. For $b \rightarrow d$ transitions the SM branching fraction is suppressed by an order of magnitude

with respect $b \rightarrow s$ processes due to a $|V_{td}|^2/|V_{ts}|^2$ factor, hence they are sensitive to more subtle effects.

The $B_{(s)}^0 \rightarrow VV'$ penguin modes, where V and V' are light vector mesons, are ideal channels to understand the physics of B mesons hadronic decays since they involve three amplitudes as compared to single amplitude $B_{(s)}^0$ penguin decays into two pseudoscalars. There are five modes in this category. Three of them: $B^0 \rightarrow \phi K^{*0}$, $B_s^0 \rightarrow \phi\phi$ and $B_s^0 \rightarrow K^{*0}\bar{K}^{*0}$ are $b \rightarrow s$ penguins whereas there are two penguin decay modes that correspond to $b \rightarrow d$ transition loops: the $B_s^0 \rightarrow \phi K^{*0}$ decay, recently discovered [16], and the $B^0 \rightarrow K^{*0}\bar{K}^{*0}$ decay, that remains controversial to date since the BaBar collaboration reported its discovery with 6σ significance and a measurement of its branching fraction of $\mathcal{B}(B^0 \rightarrow K^{*0}\bar{K}^{*0}) = (1.28_{-0.30}^{+0.35} \pm 0.11) \times 10^{-6}$ [17] whereas the Belle collaboration established an upper limit of $\mathcal{B}(B^0 \rightarrow K^{*0}\bar{K}^{*0}) < 0.8 \times 10^{-6}$ at the 90% confidence level [18].

In this document the recent progress achieved by LHCb in the understanding on two of these channels, the $B^0 \rightarrow \phi K^{*0}$ and $B_s^0 \rightarrow \phi\phi$ modes, is presented.

3.1 Angular analysis of the $B^0 \rightarrow \phi K^{*0}$ decay

The decay involves a spin-0 B -meson decaying into two spin-1 vector mesons ($B^0 \rightarrow VV'$). Due to angular momentum conservation there are only three independent configurations of the final-state spin vectors: a longitudinal component and two transverse components with collinear and orthogonal polarisations. Previous angular analyses have shown that the longitudinal and transverse components in this decay have roughly equal amplitudes, similarly to other $B_{(s)}^0 \rightarrow VV'$ penguin transitions [19]. Naïvely, given the V–A structure of the weak interaction, and as observed in $b \rightarrow u$ tree level processes [20], the longitudinal polarisation should dominate. The different behaviour of tree and penguin decays has attracted much theoretical attention, with several explanations proposed such as large contributions from penguin annihilation effects [21] or final-state interactions [22]. More recent calculations based on QCD factorisation [23] are consistent with the data, although with significant uncertainties.

The selection of events in LHCb 2011 data is structured into a first part of rectangular cuts followed by a multivariate method. The sensitive variables select groups of four large impact parameter tracks that define a good quality secondary vertex with positive identification of three kaons and one pion. The resulting charged particles are combined to form ϕ and K^{*0} meson candidates. The invariant mass of the K^+K^- ($K^+\pi^-$) pair is required to be within $\pm 15 \text{ MeV}/c^2$ ($\pm 150 \text{ MeV}/c^2$) of the known mass of the ϕ (K^{*0}) meson. With these cuts a total of 1852 signal events are selected.

These data are analysed with a 5-dimensional unbinned maximum likelihood fit in the two-body masses and the polarisation angles. The angle prescription is described in Figure 3.1. As a result of the fit a longitudinal polarisation fraction of $0.497 \pm 0.019 \text{ stat} \pm 0.015 \text{ syst}$ is obtained, the most precise measurement to date.

This is a self-tagged mode. Thus, the flavor of the b (or \bar{b}) quark at production is measured with the charge of the decay products of the K^{*0} (\bar{K}^{*0}). Therefore, the different yields of B^0 and \bar{B}^0 decays can be determined. The asymmetry between these yields is measured relative to the $B^0 \rightarrow J/\psi K^{*0}$ control channel, cancelling detector and production asymmetries, and is found to

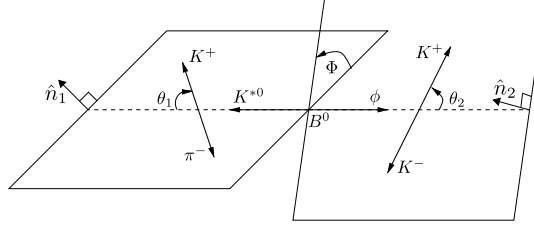


Figure 2: The helicity angles θ_1 , θ_2 , Φ for the $B^0 \rightarrow \phi K^{*0}$ decay.

Table 2: Comparison of measurements made by the LHCb, BaBar [24] and Belle [25] collaborations. The first uncertainty is statistical and the second systematic. The longitudinal and perpendicular polarisation fractions f_L , and f_\perp , are displayed, as well as the relative phases of the longitudinal and parallel amplitudes with respect to the longitudinal δ_\perp and δ_\parallel and the CP asymmetries of the polarisation amplitude sizes and phases.

| Parameter | LHCb | BaBar | Belle |
|-------------------------|------------------------------|-----------------------------|------------------------------|
| f_L | $0.497 \pm 0.019 \pm 0.015$ | $0.494 \pm 0.034 \pm 0.013$ | $0.499 \pm 0.030 \pm 0.018$ |
| f_\perp | $0.221 \pm 0.016 \pm 0.013$ | $0.212 \pm 0.032 \pm 0.013$ | $0.238 \pm 0.026 \pm 0.008$ |
| δ_\perp | $2.633 \pm 0.062 \pm 0.037$ | $2.35 \pm 0.13 \pm 0.09$ | $2.37 \pm 0.10 \pm 0.04$ |
| δ_\parallel | $2.562 \pm 0.069 \pm 0.040$ | $2.40 \pm 0.13 \pm 0.08$ | $2.23 \pm 0.10 \pm 0.02$ |
| A_0^{CP} | $-0.003 \pm 0.038 \pm 0.005$ | $+0.01 \pm 0.07 \pm 0.02$ | $-0.030 \pm 0.061 \pm 0.007$ |
| A_\perp^{CP} | $+0.047 \pm 0.072 \pm 0.009$ | $-0.04 \pm 0.15 \pm 0.06$ | $-0.14 \pm 0.11 \pm 0.01$ |
| δ_\perp^{CP} | $+0.062 \pm 0.062 \pm 0.006$ | $+0.21 \pm 0.13 \pm 0.08$ | $+0.05 \pm 0.10 \pm 0.02$ |
| δ_\parallel^{CP} | $+0.045 \pm 0.068 \pm 0.015$ | $+0.22 \pm 0.12 \pm 0.08$ | $-0.02 \pm 0.10 \pm 0.01$ |

be:

$$\Delta A_{CP} = (+1.5 \pm 3.2 \text{ stat} \pm 0.5 \text{ syst}) \%$$

The amplitudes and phases of the angular analysis can be used to calculate triple-product asymmetries [26]. Non-zero triple-product asymmetries arise either due to a T violating phase or a CP conserving phase and final-state interactions. Assuming CPT symmetry, a T violating phase implies that CP is violated.

For the P-wave decay, two triple-product asymmetries are calculated from the results of the angular analysis,

$$A_U = \frac{\Gamma(s_{\theta_1\theta_2} \sin \Phi > 0) - \Gamma(s_{\theta_1\theta_2} \sin \Phi < 0)}{\Gamma(s_{\theta_1\theta_2} \sin \Phi > 0) + \Gamma(s_{\theta_1\theta_2} \sin \Phi < 0)} \quad \text{and} \quad A_V = \frac{\Gamma(\sin 2\Phi > 0) - \Gamma(\sin 2\Phi < 0)}{\Gamma(\sin 2\Phi > 0) + \Gamma(\sin 2\Phi < 0)},$$

where $s_{\theta_1\theta_2} = \text{sign}(\cos \theta_1 \cos \theta_2)$.

The measured values triple-product values of LHCb 2011 data give: $A_U = -0.007 \pm 0.012 \text{ stat} \pm 0.002 \text{ syst}$ and $A_V = +0.004 \pm 0.014 \text{ stat} \pm 0.002 \text{ syst}$, compatible with the absence of CP violation.

3.2 Measurement of CP violation in $B_s^0 \rightarrow \phi\phi$ decays

This is another loop dominated process (penguin) whose angular analysis can probe new physics. Additionally, the final state of this mode is shared by B_s^0 and \bar{B}_s^0 mesons and this enables

Table 3: Results of the time dependent analysis of the $B_s^0 \rightarrow \phi\phi$ decay with statistical and systematic uncertainties.

| Parameter | Value |
|----------------|-----------------------------|
| ϕ_s (rad) | $-0.17 \pm 0.15 \pm 0.03$ |
| $ \lambda $ | $1.04 \pm 0.07 \pm 0.03$ |
| f_L | $0.364 \pm 0.012 \pm 0.009$ |
| f_\perp | $0.305 \pm 0.013 \pm 0.005$ |

Table 4: The triple-product asymmetries found from the time integrated fit. Systematic uncertainties are also quoted.

| Parameter | Value |
|-----------|------------------------------|
| A_U | $-0.003 \pm 0.017 \pm 0.006$ |
| A_V | $-0.017 \pm 0.017 \pm 0.006$ |

the interference between the decay and the decay after mixing, where mixing means the conversion of a B_s^0 into a \bar{B}_s^0 (and vice versa) through a box diagram mediated by the exchange of two virtual W bosons.

This interference permits the access to an observable phase $\phi_s = -2\beta_s = \Phi_M - 2\Phi_D$, where Φ_M is the phase shift accumulated after the mixing and Φ_D after the decay. The SM has a small prediction for $\phi_s = 0.01 \pm 0.02$ [27] due to the cancellation between the decay and mixing phases. This observable is very sensitive to the presence of new physics that may enter in the mixing loop. Direct CP violation is also possible in this decay mode since the parameter $\lambda = |p\bar{A}/qA|$ is accessible.³

The results presented in the Beauty 2014 conference correspond to the whole data sample of the LHC Run-I, thus 1 fb^{-1} at $\sqrt{s} = 7 \text{ TeV}$ of 2011 data and 1 fb^{-1} at $\sqrt{s} = 8 \text{ TeV}$ of 2012 data. The analysis supersedes the previous results presented with the 2011 data only in [28]. The signal selection has been re-optimised producing a yield of 3950 signal candidates thus, 4.5 times as many events as in the previous analysis. This is a clean mode, due to the narrowness of the two ϕ resonances, and suffers only little pollution from combinatorial combinations of four kaons and misidentified $\Lambda_b^0 \rightarrow \phi p K$ and $B^0 \rightarrow \phi K^{*0}$ decays.

The methodology of the study implements a 4-dimension, three polarisation angles plus time, tagged analysis unbinned maximum likelihood fit of the data. Some of the physical parameters of the model probability density function are taken from other analyses, such as the decay rate average Γ_s and the decay rate difference between the B_s^0 mass eigenstates $\Delta\Gamma_s$ from $B_s^0 \rightarrow J/\psi K^+ K^-$ and $B_s^0 \rightarrow J/\psi \pi^+ \pi^-$ decays [29], and the mass difference between these eigenstates Δm_s from the $B_s^0 \rightarrow D_s^- \pi^+$ mode [30]. The time resolution is obtained from simulation and calibrated on data, and found to be $\sigma_t \sim 43 \text{ fs}$. The angular acceptance is also obtained from simulation whereas the time acceptance is modelled using data from the $B_s^0 \rightarrow D_s^- \pi^+$ decay.

The results from the study, displayed in Table 3, show that no large CP violation is present in the $B_s^0 - \bar{B}_s^0$ mixing nor in the $b \rightarrow s\bar{s}s$ amplitude λ . The angular parameters demonstrate that the longitudinal polarisation is low, showing agreement with QCD factorisation predictions and disfavours the estimates of perturbative QCD. Finally, an independent time integrated fit allows the determination of triple products. In this non self-tagged mode non-zero triple products indicate different CP violating phases for CP even ($0, ||$) and CP odd (\perp) eigenstates. Also, for this case the obtained measurement is compatible with zero, as shown in Table 4.

³Here A is the amplitude of the $B_s^0 \rightarrow \phi\phi$ decay, \bar{A} the amplitude of $\bar{B}_s^0 \rightarrow \phi\phi$ and p and q are the coordinates of the mass eigenstates in the flavor eigenstates basis.

References

- [1] N. Cabibbo, Phys. Rev. Lett. **10** (1963) 531. M. Kobayashi and T. Maskawa, Prog. Theor. Phys. **49** (1973) 652.
- [2] R. Aaij *et al.* [LHCb collaboration], to appear in New J. Phys. arXiv:1407.7704 [hep-ex].
- [3] R. Aaij *et al.* [LHCb collaboration], JHEP **1405** (2014) 069.
- [4] R. Aaij *et al.* [LHCb collaboration], Phys. Rev. D **90** (2014) 052011.
- [5] A. A. Alves, Jr. *et al.* [LHCb collaboration], JINST **3** (2008) S08005.
- [6] R. Aaij *et al.* [LHCb VELO group collaboration], JINST **9** (2014) 09007. R. Arink *et al.* [LHCb Outer Tracker group collaboration], JINST **9** (2014) 01002.
- [7] M. Adinolfi *et al.* [LHCb RICH group collaboration], Eur. Phys. J. C **73** (2013) 2431.
- [8] A. A. Alves *et al.* [LHCb Muon System group collaboration], JINST **8** (2013) P02022.
- [9] J. P. Lees *et al.* [BaBar collaboration], Phys. Rev. D **87** (2013) 5, 052009. Y.-T. Duh *et al.* [Belle collaboration], Phys. Rev. D **87** (2013) 031103. R. Aaij *et al.* [LHCb collaboration], Phys. Rev. Lett. **110** (2013) 22, 221601. T. A. Aaltonen *et al.* [CDF collaboration], arXiv:1403.5586 [hep-ex].
- [10] A. Garmash *et al.* [Belle collaboration], Phys. Rev. Lett. **96** (2006) 251803. B. Aubert *et al.* [BaBar collaboration], Phys. Rev. D **78** (2008) 012004. J. P. Lees *et al.* [BaBar Collaboration], Phys. Rev. D **85** (2012) 112010. R. Aaij *et al.* [LHCb collaboration], Phys. Rev. Lett. **111** (2013) 101801. R. Aaij *et al.* [LHCb collaboration], Phys. Rev. Lett. **112** (2014) 1, 011801. R. Aaij *et al.* [LHCb collaboration], arXiv:1408.5373 [hep-ex].
- [11] R. H. Dalitz, Phil. Mag. **44** (1953) 1068.
- [12] M. Ciuchini, M. Pierini and L. Silvestrini, Phys. Rev. D **74** (2006) 051301; Phys. Lett. B **645** (2007) 201. M. Gronau, D. Pirjol, A. Soni and J. Zupan, Phys. Rev. D **75** (2007) 014002; Phys. Rev. D **77** (2008) 057504 [Addendum-ibid. D **78** (2008) 017505]. I. Bediaga, G. Guerrer and J. M. de Miranda, Phys. Rev. D **76** (2007) 073011. M. Gronau, D. Pirjol and J. Zupan, Phys. Rev. D **81** (2010) 094011.
- [13] R. Aaij *et al.*, [LHCb collaboration], Phys. Lett. B **694** (2010) 209.
- [14] Y. Amhis *et al.* [HFAG collaboration], arXiv:1207.1158 [hep-ex].
- [15] X. H. Wu and D. X. Zhang, Phys. Lett. B **587** (2004) 95. Z. J. Xiao, C. S. Li and K. T. Chao, Phys. Rev. D **63** (2001) 074005. W. J. Zou and Z. J. Xiao, Phys. Rev. D **72** (2005) 094026.
- [16] R. Aaij *et al.* [LHCb collaboration], JHEP **1311** (2013) 092.
- [17] B. Aubert *et al.*, [BaBar collaboration], Phys. Rev. Lett. **100** (2008) 081801.
- [18] C.-C. Chiang *et al.*, [Belle collaboration], Phys. Rev. D **81** (2010) 071101.
- [19] P. del Amo Sanchez *et al.* [BaBar collaboration], Phys. Rev. D **83** (2011) 051101. J. Zhang *et al.* [Belle collaboration], Phys. Rev. Lett. **95** (2005) 141801. B. Aubert *et al.* [BaBar collaboration], Phys. Rev. Lett. **97** (2006) 201801. R. Aaij *et al.* [LHCb collaboration], Phys. Lett. B **709** (2012) 50.
- [20] A. Somov *et al.*, [Belle collaboration], Phys. Rev. D **76** (2007) 011104. B. Aubert *et al.*, [Babar collaboration], Phys. Rev. D **76** (2007) 052007. J. Zhang *et al.*, [Belle collaboration], Phys. Rev. Lett. **91** (2003) 221801. B. Aubert *et al.*, [BaBar collaboration], Phys. Rev. Lett. **102** (2009) 141802. B. Aubert *et al.*, [BaBar collaboration], Phys. Rev. D **79**, (2009) 052005.
- [21] A. L. Kagan, Phys. Lett. B **601** (2004) 151.

- [22] A. Datta, A. V. Gritsan, D. London, M. Nagashima and A. Szykman, Phys. Rev. D **76** (2007) 034015.
- [23] M. Beneke, J. Rohrer and D. Yang, Nucl. Phys. B **774** (2007) 64. H. Y. Cheng and C. K. Chua, Phys. Rev. D **80** (2009) 114026.
- [24] B. Aubert *et al.* [BaBar collaboration], Phys. Rev. D **78** (2008) 092008.
- [25] M. Prim *et al.* [Belle collaboration], Phys. Rev. D **88** (2013) 7, 072004.
- [26] M. Gronau and J. L. Rosner, Phys. Rev. D **84** (2011) 096013. W. Bensalem and D. London, Phys. Rev. D **64** (2001) 116003. A. Datta and D. London, Int. J. Mod. Phys. A **19** (2004) 2505.
- [27] M. Bartsch, G. Buchalla and C. Kraus, arXiv:0810.0249 [hep-ph].
- [28] R. Aaij *et al.* [LHCb collaboration], Phys. Rev. Lett. **110** (2013) 24, 241802.
- [29] R. Aaij *et al.* [LHCb collaboration], Phys. Rev. D **87** (2013) 11, 112010.
- [30] R. Aaij *et al.* [LHCb collaboration], New J. Phys. **15** (2013) 053021 [arXiv:1304.4741 [hep-ex]].